ARTICLE PREPRINT

Cell cycle-balanced expression of pluripotency regulators via cyclin-dependent kinase 1 activity

Sergo Kasvandik[1], Reelika Schilf[1], Merilin Saarma[1], Mart Loog[1], Kersti Jääger[1,2*]

[1]Institute of Technology, University of Tartu, Nooruse 1, Tartu 50411, Estonia. [2]Present address: Competence Centre on Health Technologies, Tiigi 61b, Tartu 50410, Estonia. [*]Correspondence: Kersti Jääger - kerstijaager@gmail.com

ABSTRACT

Embryonic stem cells (ESCs) have a unique ability to remain pluripotent while undergoing rapid rounds of cell division required for self-renewal. However, it is not known how cell cycle and pluripotency regulatory networks co-operate in ESCs. Here, we used stable isotope labeling with amino acids in cell culture (SILAC) combined with mass spectrometry to determine pluripotency proteome dynamics during cell cycle in mouse ESCs (mESCs). We found the S/G2M-fluctuating pluripotency transcription factors (Esrrb, Rest), chromatin regulators (Jarid2, Trim24) and proteins with E3 ligase activity (Nedd4l, Pias2) to peak in S phase. This expression balance was disrupted upon inhibition of cyclin-dependent kinase 1 activity resulting in the shift of the expression peak from S to G2M. Our results show that mESCs require Cdk1 activity to maintain high S to G2M ratio of pluripotency regulators revealing critical role of cell cycle dynamics in balancing mESC identity.

INTRODUCTION

Cell cycle and pluripotency

Embryonic stem cells (ESCs) are the best studied pluripotent stem cell system that encompasses the abilities of self-renewal and differentiation. How this ability is manifested during cell division cycle is still unclear. Mouse ESCs (mESCs) grown in serum/LIF culture conditions proliferate rapidly and spend most of their time in S phase due to untypically short G1 phase (Stead et al., 2002). The pluripotency transcription factors (TFs) including Oct4, Nanog and Esrrb (van den Berg et al., 2008; Chambers et al., 2003; Nichols et al., 1998; Niwa et al., 2000) govern the intrinsic regulatory network that via interaction with extrinsic cues determine cell fate. However, our knowledge about ESC decision-making using bulk populations best reflects TF expression and interactions present in the more dominant S phase.

Connection of pluripotency TF network with cell cycle occurs via cyclin-dependent kinase 1 (Cdk1) that along with cyclin B are key players in cell cycle regulation and particularly mitosis in eukaryotic cells. Cdk1 is indispensible for the early development of the embryo, and is required for the self-renewal of mESCs and human ESCs (Neganova et al., 2014; Zhang et al., 2011). Cdk1 inhibition has been shown to trigger abnormal transcription of Oct4 target genes in mitosis and lead to loss of pluripotency in mESCs (Kim et al., 2018).

Proteome dynamics in pluripotent cells

Some studies have reported relatively uniform expression of pluripotency TFs during cell cycle both at mRNA and protein level (Shin et al., 2016; Singh et al., 2013), while others have revealed fluctuations (Gonzales et al., 2015; Van Der Laan et al., 2014; Tsubouchi et al., 2013). Given the interconnection between ESC fate choices and cell cycle (Gonzales et al., 2015; Jääger et al., 2019; Van Oudenhove et al., 2016; Pauklin and Vallier, 2013; Petruk et al., 2017), we aimed to map mESC proteome dynamics during cell cycle on a global scale.

We used stable isotope labeling with amino acids in cell culture (SILAC) combined with mass spectrometry (MS)-based identification of proteins in G1-, S- and G2M-enriched mESCs both in untreated and Cdk1-inhibitor treated cells to reveal cell cycle coordinated dynamics of pluripotency factor expression. Our experimental design enabled quantification of ca 2500 proteins across cell cycle phases and identify major reorganisation of pluripotency network expression at S-to-G2M transition upon loss of Cdk1 activity.

EXPERIMENTAL PROCEDURES

mESC culture and stable isotope labeling with amino acids in cell culture (SILAC)

Cell cycle reporter N7-mESCs that express Cyclin B1:GFP fusion protein from an endogeneous loci (Jääger et al., 2019) were cultured on 0.1% gelatin-coated tissue culture plastic in GMEM/β-mercaptoethanol/10%FCS/LIF as described before (Smith, 1991). For stable isotope labeling with amino acids in cell culture (SILAC), N7-mESCs were cultured for two weeks in DMEM/β-mercaptoethanol/LIF w/o Arg and Lys (Gibco), supplemented with 12.5% KnockOut™ Serum Replacement (Gibco), 63 mg/L light-Arg and 147 mg/L light-Lys or 147 mg/L heavy ($^{13}C_6{}^{15}N_2$)-Lys (Lys8) (Cambridge Isotope Laboratories). N7-mESCs cultured in SILAC-media were viable and proliferated normally as evidenced under microscope at passages 3 and 5 (**Fig. S1A**).

Cell cycle sorting of labelled cells

Light-Lys (L) or heavy-Lys (H) labelled N7-mESCs were sorted into different cell cycle phase fractions using flow cytometry as in (Jääger et al., 2019). Briefly, N7-mESCs were stained with 50 uL Hoechst 33342 (50 mg/mL stock) in 10 mL SILAC medium 45 min at 37^{0}C prior to FACS-sorting using the indicated gates (**Fig. S1B**). Sorted cells (500 000 cells per fraction on average) were immediately pelleted and stored at -80^{0}C until protein sample preparation. Cyclin-dependent kinase 1 (Cdk1) activity was inhibited in heavy-Lys (H) labelled N7-mESCs in SILAC/Hoechst medium prior to FACS sorting (2h in total) using 10 uM RO3306 (Cdk1i, Axon 1530).

Sample preparation strategy for mass-spectrometry (MS) analysis

Altogether, we combined seven sorted N7-mESCs samples in two configurations. For proteome profiling in G1, S and G2M, light-Lys G1 or G2M were each mixed with heavy-Lys S phase sample 1:1 by cell number, resulting in two dual-SILAC samples G1-S and

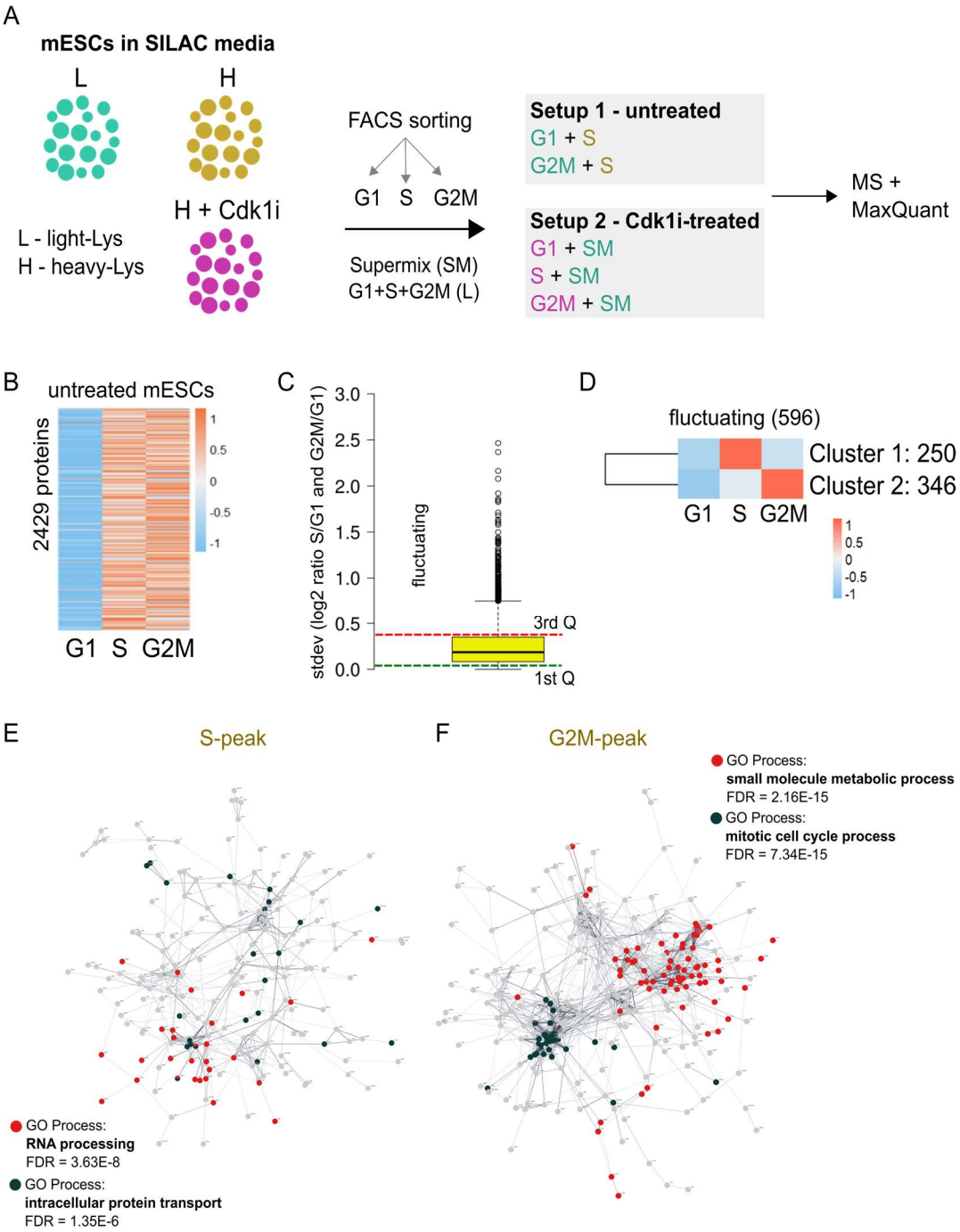

Fig. 1. mESC proteome is dynamically regulated during cell cycle. A. A schematics showing the strategy of stable isotope labeling with amino acids in cell culture (SILAC) used in combination with mass spectrometry (MS) to determine proteome dynamics during cell cycle in mouse embryonic stem cells (mESCs). Cell cycle enrichment was performed using flow cytometry sorting (**Fig. S1B**). Two MS runs were performed using the indicated sample setups 1 (untreated) and 2 (Cdk1i-treated). L = light lysine, H = heavy lysine, Cdk1i – Cyclin-dependent kinase 1 inhibitor **B.** An unclustered heatmap showing the scaled abundances of 2429 identified proteins in mESCs across cell cycle phases. **C.** Boxplot diagram showing distribution of differences (stdev-s) between S and G2M from log2 ratios of S/G1 and G2M/G1. Proteins above the red line (3rd Q) were defined as 'fluctuating' and proteins below the green line (1st Q) were defined as 'constant'. Proteins between the colored lines were defined as 'moderately changing'. **D.** Clustered abundance heatmap showing the distribution of S-G2M fluctuating proteins in C into two major clusters. Clusters were named by expression profile: S-peak (Cluster 1), G2M-peak (Cluster 2). **E and F.** Protein interaction networks of either S- or G2M-peaking protein sets derived from Cytoscape/stringApp analyses using edge-weighted network layouts. Edges represent protein-protein associations based on both experimental and indirect evidence. Unassociated proteins were excluded (S-peak: 42 proteins; G2M-peak: 47 proteins). Note sparsely interconnected network of S-peaking proteins in contrast to dense clustering in G2M-peaking protein set. Highly enriched GO Process terms were derived via STRING enrichment analysis.

G2M-S (Setup 1, **Fig. 1A**); for proteome profiling in G1, S and G2M each treated with Cdk1i, we mixed heavy-Lys G1 or S or G2M each with light-Lys supermix (SM, containing equal amount of G1-S-G2M) 1:1 by cell number, which resulted in three dual-SILAC samples G1-Cdk1i-SM, S-Cdk1i-SM, G2M-Cdk1i-SM (Setup 2, **Fig. 1A**). Detailed description of the proteomic methods can be found in **Supplementary Methods**. Briefly, cell pellets were lysed with heat and sonication in an SDS lysis buffer. Extracted proteins were methanol-chloroform precipitated and digested in denaturing conditions with Lys-C and trypsin. Peptides were desalted and injected to a Q Exactive Plus (Thermo Fisher Scientific) nano-LC MS/MS system operated in a data-dependent acquisition mode. MS raw data were identified and quantified with the MaxQuant software.

Profiling and enrichment analysis of proteomics data

The quantitative information from dual-SILAC measurements was integrated via either common S phase in setup 1 or via common super-mix (SM) in setup 2 to enable comparison between phases. Protein intensities were therefore normalised to S phase replicate 1 in setup 1 or SM replicate 1 in setup 2. Only proteins that were identified in all five standard samples (two S phase replicates and three SM replicates) were retained (2434 proteins). For plotting S phase intensities, we used the average of two replicates.

To determine highly fluctuating proteins in untreated N7-mESCs between S and G2M, the S/G1 and G2M/G1 ratios were calculated, log transformed and standard deviation (stdev) computed. 5 more proteins that were missing in both G1 and G2M were removed, leaving 2429 proteins for expression analyses. Proteins that formed the 3rd (upper) quartile on box plots statistics of stdev-s were defined as highly fluctuating between S and G2M. The 1st (lower) quartile were defined constant, and all others were defined as moderately changing. These proteins were profiled in a similar manner in Cdk1i-treated samples using S-Cdk1i/G1-Cdk1i and G2M-Cdk1i/G1-Cdk1i ratios.

For profiling of known mitotic marker proteins, we used Cyclebase mitotic signature based on both 'peaktime' and 'phenotype' associated with M phase (Santos et al., 2015). For protein interaction network analyses, we used STRING database (Snel et al., 2000; Szklarczyk et al., 2019) via Cytoscape/stringApp (Doncheva et al., 2019). Network layouts were created with 'edge-weighted spring embedded' algorithm applied to all nodes according to STRING score, and nodes colored by GO terms derived via STRING enrichment in Cytoscape (Shannon et al., 2003). Boxplots were generated with BoxPlotR web-tool (http://shiny.chemgrid.org/boxplotr/). Heatmap visualisation and k-means correlation clustering were performed in R using *pheatmap* (https://cran.r-project.org/web/packages/pheatmap/index.html). Venn diagram was generated using Venny 2.1.0 (https://bioinfogp.cnb.csic.es/tools/venny/). Barplots and lineplots were constructed either in Excel or R using *ggplot2*.

RESULTS

mESC proteome is dynamically regulated during cell cycle

To measure relative protein abundances in mESCs during cell cycle, we enriched isotope-labelled cell cycle reporter N7-mESCs (Jääger et al., 2019) for G1, S and G2M phases using flow cytometry (**Fig. S1B**), and prepared two dual-SILAC samples where S phase standard was combined with either G1 or G2M (**Fig. 1A**). This strategy enabled G1-S-G2M normalisation via S phase and direct inter-sample comparison, resulting in relative quantification of 2429 proteins during mESC cell cycle (**see Material and methods, Suppl. Table 1**).

First, by global profiling of protein expression during cell cycle, we determined profound increase in overall protein abundances both in S and G2M compared with G1 (**Fig. 1B**). This pattern may reflect increase in cell size towards S/G2M. However, as the active maintenance of pluripotency occurs in S and G2M phases (Gonzales et al., 2015), we were particularly interested in determining dynamic changes at this transition. To enable direct comparison between S and G2M, we used G1 as a reference and computed log2 ratios for S/G1 and G2M/G1. Expression of the mitotic signature genes obtained from Cyclebase (Santos et al., 2015) confirmed gradual increase in towards G2M (>log2-fold increase, G2M versus G1)(**Fig. S2A**), and therefore the capture of known cell cycle dynamics.

To identify groups of proteins with characteristic S/G2M dynamics, we calculated standard deviations (stdev) between log2 ratios of S/G1 and G2M/G1 and used box plot diagrams of stdev-s to classify proteins into fluctuating (upper 3rd quartile, Q), constant (lower 1st Q) and moderately changing (the middle 50%) (**Fig 1C, Suppl. Table 2**), a strategy previously used for cell cycle proteomics in yeast (Carpy et al., 2014). We focussed our analysis on the fluctuating proteome (596 proteins) and aimed to determine the direction of the change. K-means correlation clustering into two major clusters revealed 250 proteins to peak in S (Cluster 1) and 346 proteins to peak in G2M (Cluster 2) (**Fig. 1D**, **Suppl. Table 2**). This analysis shows that slightly larger proportion of fluctuating proteins (58%) peak in G2M.

Gene ontology (GO) analysis using DAVID (Huang et al., 2009) revealed that the S phase-peaking protein set (Cluster 1) was enriched for biological processes related to transcription and protein transport (**Fig. S2B**), whereas processes overrepresented in G2M-peaking set (Cluster 2) included cell divison and oxidation-reduction process, in line with cell cycle features. Protein interaction network analysis using STRING (Snel et al., 2000; Szklarczyk et al., 2019) identified sparsely connected topology amongst S-peaking proteins (**Fig. 1E**), while proteins peaking in G2M formed dense association clusters of 'mitotic cell cycle process' and 'small molecule metabolic process' (**Fig. 1F**), in accordance with DAVID analysis (**Fig. S2B**). Overall, these results show that while major increase in global proteome abundance occurs at G1-to-S transition, the expression profiles dynamically change both from low to high and high to low at S/G2M.

Fluctuating pluripotency regulators peak in S phase

Next, we set out to determine the S/G2M dynamics of known pluripotency factors. We used PluriNet database of 292 curated pluripotency network components (Som et al., 2010) and searched for their entry in our cell cycle proteome. Altogether, 97 pluripotency factors were in our list, enabling us to determine cell cycle profile for 33% of the PluriNet (**Fig. 2A, Suppl. Table 3**). Although we did not detect the core pluripotency factors (eg Oct4, Sox2 or Nanog) in our cell cycle proteomic dataset, probably due to no nuclear enrichment (Hurrell et al., 2019), we were able to measure the abundances of several critical pluripotency regulators including Sall4, Esrrb, Fbxo15, Rest, Sall1, Zfp57, Dppa4 and Stat3, and establish their cell cycle profile in mESCs. In addition to TFs, many of the detected proteins are part of a larger pluripotency network (van den Berg et al., 2010; Gagliardi et al., 2013), and belong to chromatin-modifying complexes largely involved in mediating transcriptional repression (**Suppl. Table 3).** Correlation clustering (k-means = 3) distributed 21 pluripotency regulators into

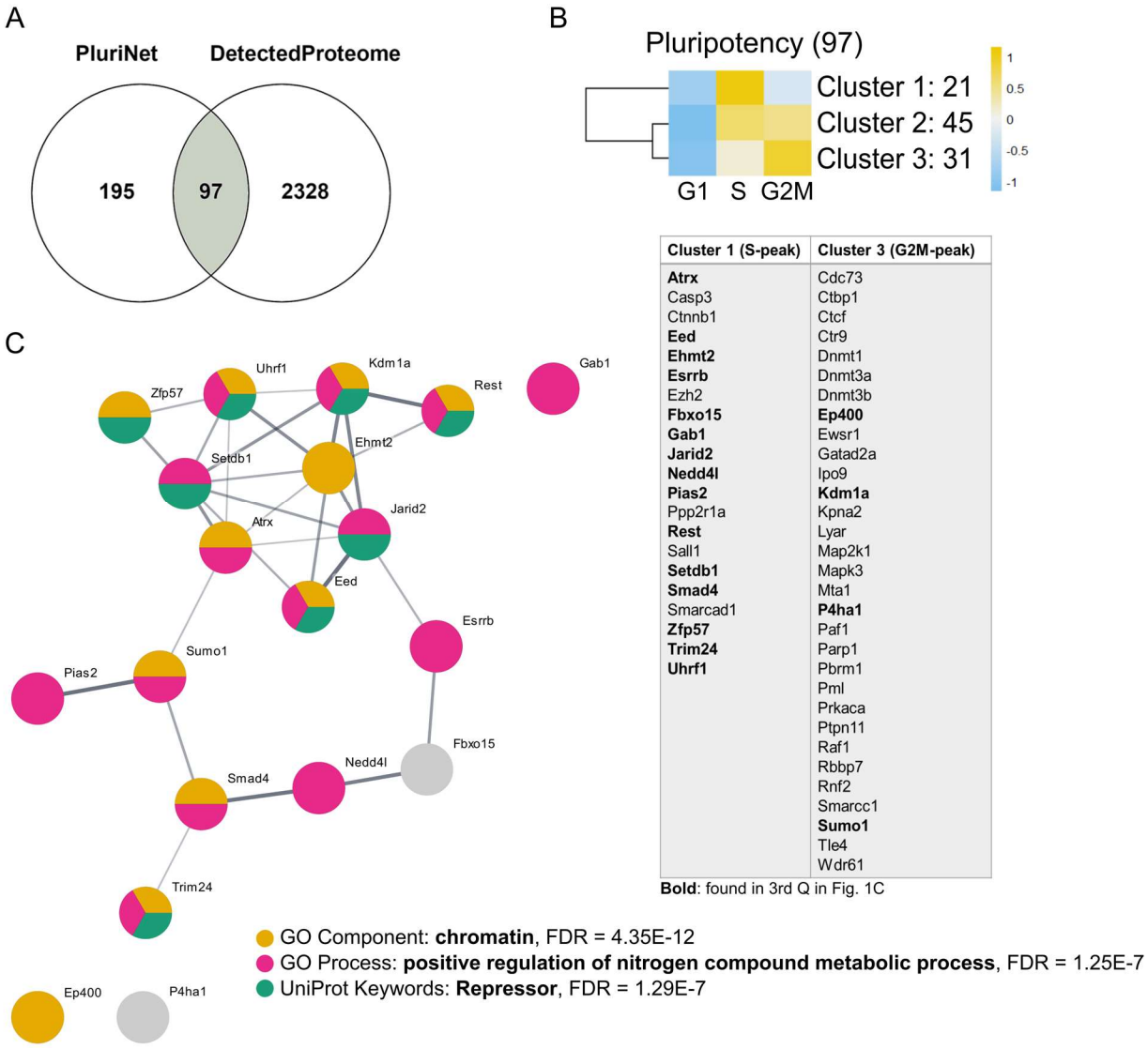

Cluster 1 (S-peak)	Cluster 3 (G2M-peak)
Atrx	Cdc73
Casp3	Ctbp1
Ctnnb1	Ctcf
Eed	Ctr9
Ehmt2	Dnmt1
Esrrb	Dnmt3a
Ezh2	Dnmt3b
Fbxo15	**Ep400**
Gab1	Ewsr1
Jarid2	Gatad2a
Nedd4l	Ipo9
Pias2	**Kdm1a**
Ppp2r1a	Kpna2
Rest	Lyar
Sall1	Map2k1
Setdb1	Mapk3
Smad4	Mta1
Smarcad1	**P4ha1**
Zfp57	Paf1
Trim24	Parp1
Uhrf1	Pbrm1
	Pml
	Prkaca
	Ptpn11
	Raf1
	Rbbp7
	Rnf2
	Smarcc1
	Sumo1
	Tle4
	Wdr61

Bold: found in 3rd Q in Fig. 1C

Fig. 2. Fluctuating pluripotency regulators peak in S phase. A. Venn diagram showing the overlap between pluripotency network (PluriNet) gene list and the proteins quantified in this study. **B.** Clustered expression heatmap showing the distribution of 97 pluripotency regulators into three major clusters: S-peaking (Cluster 1), Constant (Cluster 2) and G2M-peaking (Cluster 3). Proteins in Clusters 1 and 3 are shown in the table below. Bold marks proteins found in the 3rd Q in Fig 1C. Note predominant peaking of fluctuating proteins in S phase (15 in S versus 4 in G2M). **C.** Protein interaction network of fluctuating pluripotency regulators derived from Cytoscape/stringApp analysis using edge-weighted layout. Three proteins (Ep400, P4ha1, Gab1) were not connected to the network. Overrepresented GO terms were derived via STRING enrichment analysis.

Cluster 1 (S-peak), 45 into Cluster 2 (uniform) and 31 into Cluster 3 (G2M-peak) (**Fig. 2B)**. Pluripotency factors highlighted (bold) in the table below (**Fig. 2B)** were among the 3rd Q in Fig 1C, and were considered fluctuating (**Fig. S3A**).

Several TFs critical for mESC pluripotency including Esrrb, Rest, Atrx and Zfp57 as well as components of the Polycomb repressor complex (eg Eed, Ehmt2, Jarid2) and E3 protein ligases (eg Nedd4l, Pias2, Uhfr1) were fluctuating between S and G2M, and their abundance almost exclusively peaked in S phase (15/19) (**Fig. S3B**). Moderately changing TFs included Dppa4, Sall1, Sall4, Stat3, Ctnnb1 and proteins mediating DNA methylation (eg Dnmt1, Dnmt3a, Dnmt3b, Dnmt3l, Tet1) (**Fig. S3C**). Pluripotency regulators not changing abundance between S and G2M (constant) included TFs (Rbpj, Ctbp2, Hells) and subunits of the NuRD transcriptional repressor complex (Chd4, Hdac2, Mta2) (**Fig. S3D)**.

STRING network and enrichment analysis of the fluctuating pluripotency factors revealed overrepresentation of GO terms ‘chromatin’ and ‘positive regulation of nitrogen compound metabolic process’, and strong association between proteins enriched for ‘repressor’ activity (**Fig. 2C).** These results reveal variable cell cycle expression profile for different groups of TFs and

repressor complexes in mESCs and suggest that S-phase peaking of some key pluripotency TFs and Polycomb repressors could reflect fine coordination of pluripotency factor expression with cell cycle dynamics essential for pluripotent identity.

Inhibition of Cdk1 activity induces accumulation of cell cycle fluctuating pluripotency regulators in G2M

Given the intimate connection between pluripotency state and cell cycle dynamics, and direct modulation of pluripotency by Cdk1 in mESCs aside from its role in cell cycle regulation (Neganova et al., 2014; Wang et al., 2017), we set out to determine the sensitivity of cell cycle profile of pluripotency regulators to perturbation of Cdk1 activity. mESC cell cycle fractions treated with Cdk1 inhibitor (Cdk1i, 10 uM RO3306, 2 hours) were each measured in a 1:1 sample mix using a common standard (SM, Setup 2, **Fig. 1A, see Material and methods, Suppl. Table 4**).

On global scale, similar ratio of proteins had relatively lower abundance (negative z-score) in G1 both in untreated and Cdk1i-treated cells (ratio 0.98 vs 0.83, **Fig. S4A and B**) confirming little impact of Cdk1 in G1. Also, the ratio of proteins with positive z-scores was similarly reduced in S and G2M upon Cdk1i-treatment (from 0.87 to 0.66 in S, and from 0.88 to 0.73 in G2M), suggesting partial control of global abundances by Cdk1 in S/G2M (**Fig. S4A and B).** Importantly, mitotic proteins showed unchanged cell cycle dynamics upon Cdk1i treatment (**Fig. S4C**), confirming that Cdk1 inhibition did not induce general aberrations in mESC

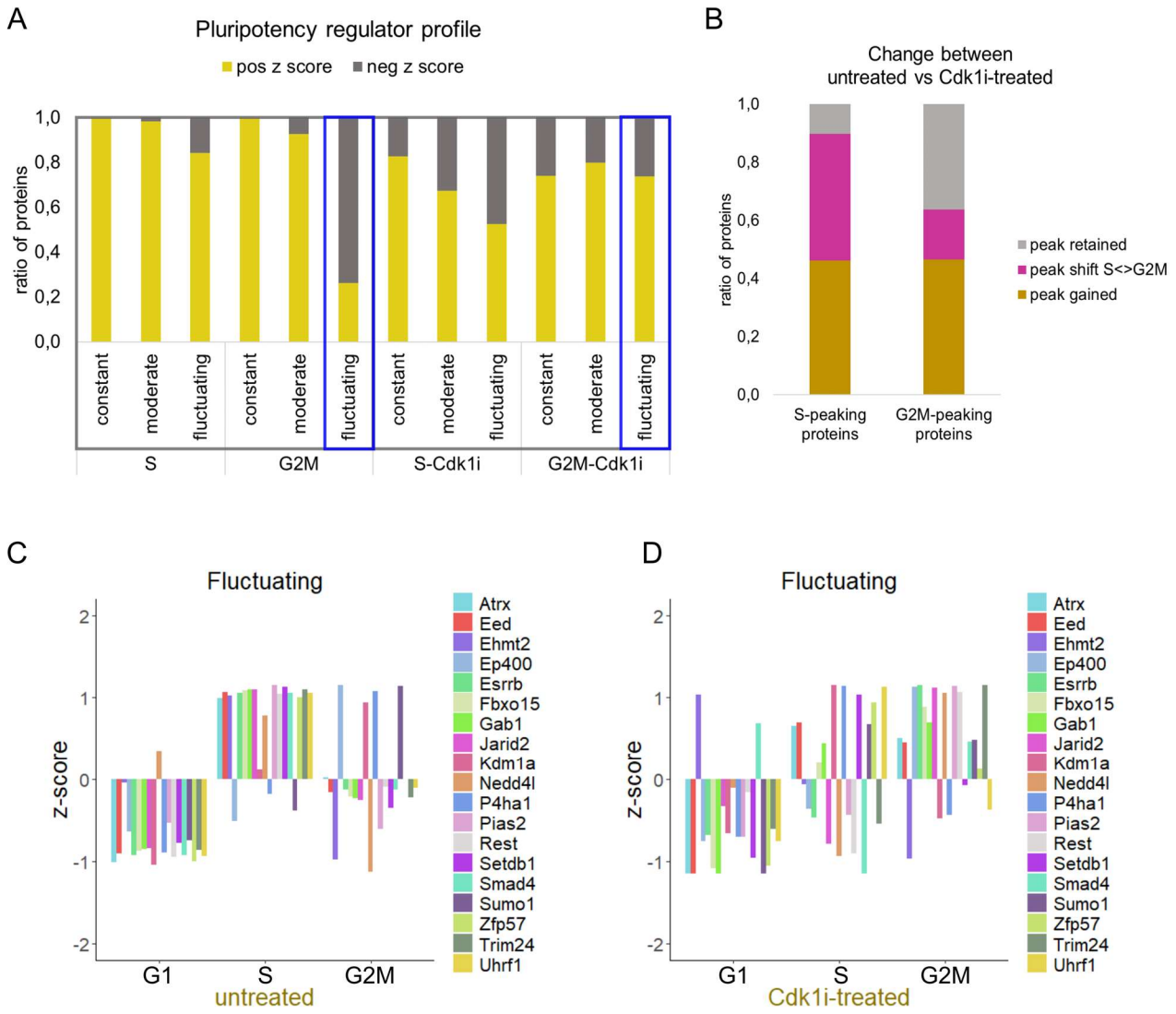

Fig. 3. Cdk1i induces accumulation of cell cycle fluctuating pluripotency regulators in G2M. A. Ratios of pluripotency regulators with either positive or negative z score in untreated and Cdk1i-treated mESCs in S and G2M phase. Note the increase in the fraction of fluctuating pluripotency regulators with positive z score upon Cdk1i-treatment in G2M phase, highlighted with blue rectangle. **B.** S- and G2M-peaking proteins (from Fig. S3B) grouped by change between untreated and Cdk1i-treated mESCs. **C and D**. Barplots showing expression dynamics of the fluctuating pluripotency regulators in untreated (C) and Cdk1i-treated (D) mESCs between cell cycle phases. Note the reorganisation of expression profiles in S and G2M.

cell cycle. Analysis of the response of 596 globally fluctuating proteins to Cdk1i showed that roughly half of the S- and G2M-peaking proteins shifted peak between S and G2M (**Fig. S4D**). Cdk1i-sensitive proteins in S-peaking set were related to 'transcription', and in G2M-peaking set to 'oxidation-reduction' and 'metabolic process' as revealed via GO analysis (**Fig. S4E**), while the Cdk1i-insensitive processes were related to DNA damage and repair in S phase, and cell division in G2M (**Fig. S4E**), suggesting relevant role of Cdk1 in balancing protein expression between S and G2M in mESCs in addition to classical cell cycle regulation.

Next, to determine the balance of pluripotency factor expression during cell cycle in response to Cdk1i treatment, we compared proteins by grouping into constant, moderately changing and fluctuating as in Fig. S3A (**Fig. 3A**). This analysis revealed general reduction in the ratio of proteins with positive z-scores upon Cdk1 inhibition in S phase. Interestingly, similar pattern was seen for 'constant' and 'moderate' groups of proteins in G2M but not for the 'fluctuating' group where the ratio of proteins with positive z-score increased from 0.26 to 0.74 upon Cdk1i treatment (blue rectangle in **Fig. 3A),** suggesting pluripotency factor accumulation in G2M in response to Cdk1. Indeed, a considerable fraction of S-peaking pluripotency regulators (0.44) showed peak shift from S to G2M (**Fig. 3B),** resulting in reorganisation of S/G2M balanced expression of pluripotency factors (**Fig. 3C)** when Cdk1 activity was inhibited **(Fig. 3D).**

Differential sensitivity of pluripotency regulators to inhibition of Cdk1 activity

Finally, we visualised three groups of fluctuating pluripotency factors from Fig. 3C and D according to cell cycle profiles to enable a more detailed investigation of changes between S and G2M (**Fig. 4A-C**). TFs Esrrb and Rest, chromatin regulators Jarid2 and Trim24, and E3 ligases Nedd4l and Pias2 all switched their maximal levels from S to G2M upon Cdk1i (**Fig. 4A).** Another group of regulators including Atrx, Eed, Fbxo15 and Gab1 lost the characteristic peak in S and gained uniform expression between S and G2M when Cdk1 activity was inhibited (**Fig. 4B).** A few pluripotency regulators including Setdb1, Zfp57 and Uhfr1 were insensitive to Cdk1i and retained high S to G2M ratio (**Fig. 4C).**

Together, our results show that the majority of pluripotency factors is not uniformly expressed between S and G2M, and reveal a highly fluctuating group of proteins particularly sensitive to Cdk1 inhibition at S/G2M.

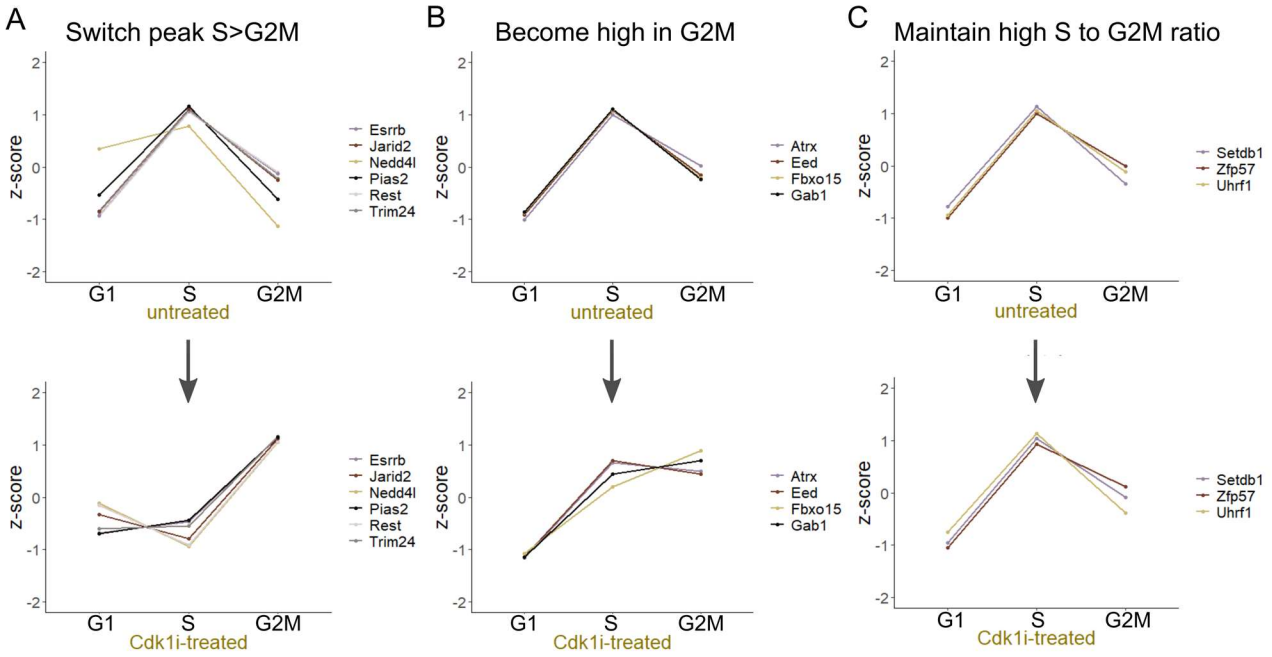

Fig. 4. Differential sensitivity of pluripotency regulators to Cdk1i treatment. A-C. Lineplots showing expression dynamics of different groups of pluripotency regulators either switching peak from S to G2M (eg Esrrb, Jarid2, Rest in A), becoming uniformly expressed in S and G2M (eg Eed, Fbxo15 in B) or being insensitive to Cdk1 inhibition (eg Setdb1, Zfp57 in C).

DISCUSSION

S/G2M dynamics of pluripotency regulators

ESC pluripotency relies on an intrinsic TF network that interacts with extrinsic signals to direct fate choices. Cell cycle phasing determines alternative ESC pluripotency states and fate choices (Gonzales et al., 2015; Jääger et al., 2019; Van Oudenhove et al., 2016; Pauklin and Vallier, 2013). In our study, we show that mESC proteome is finely balanced between S and G2M phases, and that this balance becomes disrupted upon loss of Cdk1 activity.

Chromatin regulators along with tightly regulated TF circuits play important roles in balancing self-renewal and pluripotency in ESCs (Orkin and Hochedlinger, 2011). We found the majority of S/G2M fluctuating pluripotency factors to peak in S phase. These included both critical TFs and transcriptional co-regulators. Interestingly, many factors with repressive activity were found to be particularly sensitive to cell cycle changes. The repressor proteins may be critical to deposit repressive marks temporarily after DNA replication in S phase to prevent

differentiation (Petruk et al., 2017), after which their levels need to be reduced again to enable plasticity. The same proteins that we identified here in whole cell lysates were recently found to be over-represented in the chromatin-associated fraction of the mESC proteome (van Mierlo et al., 2019). It is probable then, that via nuclear enrichment, many more pluripotency regulators including core TFs could be profiled using similar approach.

Reorganisation of S/G2M balance upon loss of Cdk1 activity

Cdk1 is essential for mESC self-renewal (Zhang et al., 2011) and downregulation of Cdk1 causes pluripotent stem cell accumulation in G2 phase, loss of pluripotency and induction of differentiation (Neganova et al., 2014). Therefore, our finding that key pluripotency TFs and co-regulators accumulate in G2M instead of S when Cdk1 activity is inhibited, suggest S-peaking to have an essential role in maintaining the pluripotent identity of mESC. Not surprisingly then, mESCs spend most of their time in S phase (Stead et al., 2002).

The reduction in expression of some pluripotency TFs including Esrrb marks mESC commitment to differentiation (Festuccia et al., 2018). Moreover, variable Esrrb levels separate distinct pluripotency states in G2M (Jääger et al., 2019). Therefore, loss of S-phase peaking of Esrrb protein upon Cdk1 inhibition may suggest that the collapse of naive pluripotency is initiated in at S phase.

We found the fluctuating proteome to be enriched for TFs and chromatin regulators with repressive functions including the polycomb complex. Cell cycle regulation of EZH2 (enzymatic component of the polycomb repressive complex 2, PRC2) via Cdk1, one of the moderately changing proteins in mESCs identified here, has been shown to have both positive and negative outcomes on stem cell identity and differentiation (Chen et al., 2010; Kaneko et al., 2010; Wei et al., 2011). Our results suggest that such opposite Cdk1-induced phenotypes could arise from cell cycle coordination of alternative Cdk1 activities in S and G2M, emphasizing the relevance of cell cycle timing in mESC fate switches.

Finally, we propose that downregulation of pluripotency markers observed in response to Cdk1 inhibition (Neganova et al., 2014) in bulk ESCs may reflect the reorganisation of abundance profiles between S and G2M observed in this study. Future investigations should address the molecular details of Cdk1-mediated control of protein expression at late cell cycle phases and its role in maintaining and/or releasing pluripotent identity of ESCs.

Conclusion

Our findings demonstrate that the expression of pluripotency regulatory network is coordinated with S/G2M transitions and it rapidly sensitises changes in Cdk1 activity.

Author Contributions and Notes

S.K. and K.J. designed research; S.K., R.S., M.S. and K.J. performed research; K.J. and S.K. analyzed data; K.J. wrote the paper with contributions from S.K. and M.L. The authors declare no conflict of interest. This article contains supplementary information online:
Supplementary_Figures.pdf
Supplementary_Methods.pdf

Acknowledgments

We thank Eve Toomsoo and Reet Kurg at Institute of Technology (TUIT) for kind assistance with cell sorting, and Mihkel Örd and Viljar Jaks for helpful discussions. We also thank Ian Chambers at University of Edinburgh for kindly sharing the N7-mESC cell line. This research was supported by the Mobilitas Pluss Programme grant (MOBTP28) in Estonia from the European Regional Development Fund. M.L. and R.S. were supported by ERC Consolidator Grant nr. 649124 PHOSPHOPROCESSORS (M.L.), Centre of Excellence for “Molecular Cell Technologies” TK143 (M.L.), Estonian Science Agency grants IUT2-21 and PRG550 (M.L.).

REFERENCES

van den Berg, D.L.C., Zhang, W., Yates, A., Engelen, E., Takacs, K., Bezstarosti, K., Demmers, J., Chambers, I., and Poot, R.A. (2008). Estrogen-Related Receptor Beta Interacts with Oct4 To Positively Regulate Nanog Gene Expression. Mol. Cell. Biol. *28*, 5986–5995.

van den Berg, D.L.C., Snoek, T., Mullin, N.P., Yates, A., Bezstarosti, K., Demmers, J., Chambers, I., and Poot, R.A. (2010). An Oct4-Centered Protein Interaction Network in Embryonic Stem Cells. Cell Stem Cell.

Carpy, A., Krug, K., Graf, S., Koch, A., Popic, S., Hauf, S., and Macek, B. (2014). Absolute proteome and phosphoproteome dynamics during the cell cycle of Schizosaccharomyces pombe (Fission Yeast). Mol. Cell. Proteomics *13*, 1925–1936.

Chambers, I., Colby, D., Robertson, M., Nichols, J., Lee, S., Tweedie, S., Smith, A., Ashfield, R., Patel, A.., Bossone, S.., et al. (2003). Functional Expression Cloning of Nanog, a Pluripotency Sustaining Factor in Embryonic Stem Cells. Cell *113*, 643–655.

Chen, S., Bohrer, L.R., Rai, A.N., Pan, Y., Gan, L., Zhou, X., Bagchi, A., Simon, J.A., and Huang, H. (2010). Cyclin-dependent kinases regulate epigenetic gene silencing through phosphorylation of EZH2. Nat. Cell Biol. *12*, 1108–1114.

Doncheva, N.T., Morris, J.H., Gorodkin, J., and Jensen, L.J. (2019). Cytoscape StringApp: Network Analysis and Visualization of Proteomics Data. J. Proteome Res. *18*, 623–632.

Festuccia, N., Halbritter, F., Corsinotti, A., Gagliardi, A., Colby, D., Tomlinson, S.R., and Chambers, I. (2018). Esrrb extinction triggers dismantling of naïve pluripotency and marks commitment to differentiation. EMBO J. *37*, e95476.

Gagliardi, A., Mullin, N.P., Ying Tan, Z., Colby, D., Kousa, A.I., Halbritter, F., Weiss, J.T., Felker, A., Bezstarosti, K., Favaro, R., et al. (2013). A direct physical interaction between Nanog and Sox2 regulates embryonic stem cell self-renewal. EMBO J. *32*, 2231–2247.

Gonzales, K.A.U., Liang, H., Lim, Y.S., Chan, Y.S., Yeo, J.C., Tan, C.P., Gao, B., Le, B., Tan, Z.Y., Low, K.Y., et al. (2015). Deterministic Restriction on Pluripotent State Dissolution by Cell-Cycle Pathways. Cell *162*, 564–579.

Huang, D.W., Sherman, B.T., and Lempicki, R.A. (2009). Systematic and integrative analysis of large gene lists using DAVID bioinformatics resources. Nat. Protoc. *4*, 44–57.

Hurrell, T., Segeritz, C.P., Vallier, L., Lilley, K.S., and Cromarty, A.D. (2019). A proteomic time course through the differentiation of human induced pluripotent stem cells into hepatocyte-like cells. Sci. Rep.

Jääger, K., Simpson, D., Kalantzaki, M., Salzano, A., Chambers, I., and Chandra, T. (2019). G2M splits mouse embryonic stem cells into naïve and formative pluripotency states. BioRxiv 616516.

Kaneko, S., Li, G., Son, J., Xu, C.-F., Margueron, R., Neubert, T.A., and Reinberg, D. (2010). Phosphorylation of the PRC2 component Ezh2 is cell cycle-regulated and up-regulates its binding to ncRNA. Genes Dev. *24*, 2615–2620.

Kim, H.J., Shin, J., Lee, S., Kim, T.W., Jang, H., Suh, M.Y., Kim, J.-H., Hwang, I.-Y., Hwang, D.S., Cho, E.-J., et al. (2018). Cyclin-dependent kinase 1 activity coordinates the chromatin associated state of Oct4 during cell cycle in embryonic stem cells. Nucleic Acids Res. *46*, 6544–6560.

Van Der Laan, S., Golfetto, E., Vanacker, J.M., and Maiorano, D. (2014). Cell cycle-dependent expression of Dub3, Nanog and the p160 family of nuclear receptor coactivators (NCoAs) in mouse embryonic stem cells. PLoS One *9*, 1–11.

van Mierlo, G., Wester, R.A., and Marks, H. (2019). A mass spectrometry survey of chromatin-associated proteins in pluripotency and early lineage commitment. Proteomics.

Neganova, I., Tilgner, K., Buskin, A., Paraskevopoulou, I., Atkinson, S.P., Peberdy, D., Passos, J.F., and Lako, M. (2014). CDK1 plays an important role in the maintenance of pluripotency and genomic stability in human pluripotent stem cells. Cell Death Dis. *5*, e1508.

Nichols, J., Zevnik, B., Anastassiadis, K., Niwa, H., Klewe-Nebenius, D., Chambers, I., Schöler, H., and Smith, A. (1998). Formation of pluripotent stem cells in the mammalian embryo depends on the POU transcription factor Oct4. Cell *95*, 379–391.

Niwa, H., Miyazaki, J., and Smith, A.G. (2000). Quantitative expression of Oct-3/4 defines differentiation, dedifferentiation or self-renewal of ES cells. Nat. Genet. *24*, 372–376.

Orkin, S.H., and Hochedlinger, K. (2011). Chromatin connections to pluripotency and cellular reprogramming. Cell *145*, 835–850.

Van Oudenhove, J.J., Grandy, R.A., Ghule, P.N., del Rio, R., Lian, J.B., Stein, J.L., Zaidi, S.K., and Stein, G.S. (2016). Lineage-Specific Early Differentiation of Human Embryonic Stem Cells Requires a G2 Cell Cycle Pause. Stem Cells *34*, 1765–1775.

Pauklin, S., and Vallier, L. (2013). The cell-cycle state of stem cells determines cell fate propensity. Cell *155*, 135–147.

Petruk, S., Cai, J., Sussman, R., Sun, G., Kovermann, S.K., Mariani, S.A., Calabretta, B., McMahon, S.B., Brock, H.W., Iacovitti, L., et al. (2017). Delayed Accumulation of H3K27me3 on Nascent DNA Is Essential for Recruitment of Transcription Factors at Early Stages of Stem Cell Differentiation. Mol. Cell *66*, 247-257.e5.

Santos, A., Wernersson, R., and Jensen, L.J. (2015). Cyclebase 3.0: a multi-organism database on cell-cycle regulation and phenotypes. Nucleic Acids Res. *43*, D1140–D1144.

Shannon, P., Markiel, A., Ozier, O., Baliga, N.S., Wang, J.T., Ramage, D., Amin, N., Schwikowski, B., and Ideker, T. (2003). Cytoscape: A Software Environment for Integrated Models of Biomolecular Interaction Networks. Genome Res. *13*, 2498.

Shin, J., Kim, T.W., Kim, H., Kim, H.J., Suh, M.Y., Lee, S., Lee, H.-T., Kwak, S., Lee, S.-E., Lee, J.-H., et al. (2016). Aurkb/PP1-mediated resetting of Oct4 during the cell cycle determines the identity of embryonic stem cells. Elife *5*, e10877.

Singh, A.M., Chappell, J., Trost, R., Lin, L., Wang, T., Tang, J., Wu, H., Zhao, S., Jin, P., and Dalton, S. (2013). Cell-cycle control of developmentally regulated transcription factors accounts for heterogeneity in human pluripotent cells. Stem Cell Reports *1*, 532–544.

Smith, A.G. (1991). Culture and differentiation of embryonic stem cells. J. Tissue Cult. Methods *13*, 89–94.

Snel, B., Lehmann, G., Bork, P., and Huynen, M.A. (2000). STRING: a web-server to retrieve and display the repeatedly occurring neighbourhood of a gene. Nucleic Acids Res. *28*, 3442–3444.

Som, A., Harder, C., Greber, B., Siatkowski, M., Paudel, Y., Warsow, G., Cap, C., Schöler, H., and Fuellen, G. (2010). The PluriNetWork: An Electronic Representation of the Network Underlying Pluripotency in Mouse, and Its Applications. PLoS One *5*, e15165.

Stead, E., White, J., Faast, R., Conn, S., Goldstone, S., Rathjen, J., Dhingra, U., Rathjen, P., Walker, D., and Dalton, S. (2002). Pluripotent cell division cycles are driven by ectopic Cdk2, cyclin A/E and E2F activities. Oncogene *21*, 8320–8333.

Szklarczyk, D., Gable, A.L., Lyon, D., Junge, A., Wyder, S., Huerta-Cepas, J., Simonovic, M., Doncheva, N.T., Morris, J.H., Bork, P., et al. (2019). STRING v11: protein–protein association networks with increased coverage, supporting functional discovery in genome-wide experimental datasets. Nucleic Acids Res. *47*, D607–D613.

Tsubouchi, T., Soza-Ried, J., Brown, K., Piccolo, F.M., Cantone, I., Landeira, D., Bagci, H., Hochegger, H., Merkenschlager, M., and Fisher, A.G. (2013). DNA synthesis is required for reprogramming mediated by stem cell fusion. Cell *152*, 873–883.

Wang, X.Q., Lo, C.M., Chen, L., Ngan, E.S.-W., Xu, A., and Poon, R.Y. (2017). CDK1-PDK1-PI3K/Akt signaling pathway regulates embryonic and induced pluripotency. Cell Death Differ. *24*, 38–48.

Wei, Y., Chen, Y.-H., Li, L.-Y., Lang, J., Yeh, S.-P., Shi, B., Yang, C.-C., Yang, J.-Y., Lin, C.-Y., Lai, C.-C., et al. (2011). CDK1-dependent phosphorylation of EZH2 suppresses methylation of H3K27 and promotes osteogenic differentiation of human mesenchymal stem cells. Nat. Cell Biol. *13*, 87–94.

Zhang, W.W., Zhang, X.J., Liu, H.X., Chen, J., Ren, Y.H., Huang, D.G., Zou, X.H., and Xiao, W. (2011). Cdk1 is required for the self-renewal of mouse embryonic stem cells. J. Cell. Biochem. *112*, 942–948.